Front. Earth Sci. 2025, 19(2): 213–231
https://doi.org/10.1007/s11707-024-1125-y

RESEARCH ARTICLE

Detecting dynamic changes in mangrove forests in the Dandou Sea, Beibu Gulf

Tianliang WU[1,2], Wenhong PANG[1], Riming WANG (✉)[1], Hu HUANG[1], Shaohan SHEN[3], Chunmei HUANG[1], Baoqing HU[2]

1 Guangxi Key Laboratory of Marine Environmental Change and Disaster in Beibu Gulf, Beibu Gulf University (Qinzhou), Qinzhou 535011, China
2 Key Laboratory of Environment Change and Resources Use in Beibu Gulf (Ministry of Education), Nanning Normal University, Nanning 530001, China
3 Shanghai Jianping High School, Shanghai 200135, China

© Higher Education Press 2024

Abstract Mangrove forests are significant ecosystems worldwide and play a crucial role in maintaining the biodiversity of intertidal zones in tropical and subtropical regions. However, most mangroves have experienced large-scale losses due to anthropogenic activities and natural stress from environmental factors. Here, the dynamic changes in mangroves in the Dandou Sea (DDS) of the Beibu Gulf between 1987 and 2021 were analyzed via multispectral satellite remote sensing data from the Google Earth Engine Platform. The results indicated that the area of mangroves in the DDS increased from 225.90 ha in 1987 to 451.76 ha in 2021. Throughout this period, the overall mangrove area in the DDS, as well as in its western and central parts, underwent a rapid growth phase from 1987 to 1996, followed by a slow growth phase from 1997 to 2011, and eventually entered a stagnation phase from 2013 to 2021. Moreover, due to the biological invasion caused by *Spartina alterniflora*, the mangrove forests in this area tended toward fragmentation. Moreover, *S. alterniflora* suppressed the spread of mangrove forests, accounting for up to 41.69% of the total loss. In a similar vein, the local high-intensity economic activities within the tidal flat accounted for 32.55% of the mangrove loss. Additionally, the expansion of aquaculture ponds and construction land directly accounted for 9.45% and 7.91% of the mangrove loss, respectively. Furthermore, the establishment of mangrove nature reserves played a positive role in the restoration and expansion of mangroves in the DDS. Our results also demonstrated that sea level rise had little impact on mangrove retreat.

Received November 29, 2023; accepted April 7, 2024

E-mail: wangriming@bbgu.edu.cn

Keywords mangrove forests, human activities, sea level rise, Dandou Sea, Google Earth Engine

1 Introduction

Mangroves, which thrive in the intertidal zones of tropical and subtropical estuaries and bays, are heat-loving, salt-tolerant, and flood-resistant. Moreover, mangroves are among the most productive ecosystems globally and the forest system with the highest carbon storage in tropical and subtropical regions (Donato et al., 2011; Morrissette et al., 2023). Mangrove forests play a pivotal role in wave attenuation, water purification, and biodiversity maintenance (Zhou et al., 2022; Afonso et al., 2023; Rull, 2023). Additionally, mangroves mitigate coastal threats posed by rising sea levels through sediment capture, which elevates the surface of tidal flats, as well as through efficient carbon sequestration (Long et al., 2022). Therefore, mangroves play a key role in global climate change and ecological conservation through carbon sequestration, biodiversity conservation, coastal protection, water purification, socioeconomic benefits, and climate change adaptation and mitigation (Getzner and Islam, 2020; Soeprobowati et al., 2024), making them an indispensable part of global ecosystems. The protection and restoration of mangroves are crucial for achieving sustainable development goals and addressing global environmental challenges (Bimrah et al., 2022). Moreover, the intertidal zones of mangrove forests are muddy and prone to sinking, and the dense branches and trunks of mangrove trees make traditional field surveys challenging and inefficient (Long et al., 2022). In contrast, remote sensing offers an efficient, long-term, and large-scale means of obtaining mangrove information

and has been widely used in studies of mangrove area statistics, ecological monitoring, biomass estimation, and spatiotemporal distribution (Tran et al., 2022). Furthermore, the Google Earth Engine (GEE), as the most advanced visual information processing cloud platform, can directly access remote sensing image data from Landsat 5 TM and Landsat 8 OLI facilitating large-scale and long-term monitoring (Gorelick et al., 2017; Amani et al., 2020).

Over recent decades, global mangrove forests have experienced significant dynamic changes. Since the 1950s, 50% of the world's mangroves have been permanently lost (Feller et al., 2010). Additionally, 40% of mangrove species have been classified as endangered (Polidoro et al., 2010). Globally, between 1996 and 2020, the world lost 524500 ha of mangroves, with Asia, the Americas, Africa, and Oceania losing 281350 ha, 126000 ha, 64760 ha, and 52440 ha, respectively (Bunting et al., 2022). On a regional scale, most areas across continents have undergone severe mangrove degradation. For instance, Australia's annual mangrove loss rate was 0.23% between 1996 and 2010 and 0.10% from 2010 to 2020 (Bunting et al., 2022; Du et al., 2023). The Malaysian Peninsula lost 40000 ha of mangroves from 1944 to 2018 (Du et al., 2023). Moreover, the Mekong Delta in Vietnam experienced a net loss of 83640 ha of mangroves from 1973 to 2020 (Phan and Stive, 2022). Furthermore, at the Rufiji-Mafia-Kilwa Marine Ramsar Site in Tanzania, Eastern Africa, there was a decrease of up to 2012 ha between 2000 and 2020 (Du et al., 2023). In the Americas, Colombia experienced a loss of 47937 ha of mangroves from 1984 to 2020 (Murillo-Sandoval et al., 2022). However, a comprehensive understanding of the reasons or dominant factors contributing to mangrove loss remains elusive. Therefore, there is an urgent need to conduct long-term studies on the dynamics of mangrove ecosystems to understand the mechanisms behind their loss, which holds significant theoretical and practical value for the protection and restoration of regional mangroves.

Against the backdrop of a global decrease in mangrove area, relevant international organizations and governments of tropical and subtropical coastal countries have placed a high emphasis on mangrove conservation and restoration, attempting to reverse the trend of continuous degradation of mangroves (Lee et al., 2019; Long et al., 2022). With the initiation of mangrove conservation and restoration efforts, several countries have witnessed a revival in their mangrove cover. Vietnam's mangroves increased by 11705 ha between 2010 and 2019 (Tinh et al., 2022). Moreover, Ecuador's mangroves showed a trend of recovery between 2010 and 2018 (Morocho et al., 2022). Additionally, between 1988 and 2018, the mangrove cover in India increased by 20.72% (Jayanthi et al., 2022), and the mangrove area in neighboring Pakistan expanded from 47722 ha in 1990 to 146359 ha in 2020 (Gilani et al., 2021). From 1986 to 2021, China's mangrove area expanded from 10835.29 to 27427.21 ha (Wang et al., 2022). Furthermore, the mangrove forests in the Nanliu River Delta in the northern Beibu Gulf (BBG) expanded from 173.5 ha in 1986 to 1044.4 ha in 2020 (Long et al., 2022), and the Maowei Sea mangroves added 997.8 ha between 1990 and 2019 (Huang et al., 2022). However, research on their dynamic changes and the mechanisms of damage to the mangrove forests along the northern coast of China's BBG remains relatively scarce. Mangroves are susceptible to external environmental disturbances during the process of recovery and expansion, which can affect or alter the evolutionary process and direction of mangrove tidal flats. Therefore, studying the dynamic changes in the recovery and expansion of mangroves is highly valuable for the conservation and restoration of these ecosystems. This is particularly true in the face of significant threats from the large-scale invasion of the exotic species *Spartina alterniflora*.

Human activities and natural stresses have strongly impacted the dynamics of mangroves (Phan and Stive, 2022; Osorio-Olvera et al., 2023). Globally, mangrove loss is positively correlated with population density (Turschwell et al., 2020). The expansion of agricultural lands and aquaculture ponds were the primary contributors to mangrove loss (Bunting et al., 2022; Tinh et al., 2022). In Vietnam, between 2010 and 2019, aquaculture ponds and farmland expansion were responsible for 43.4% and 24.8%, respectively, of mangrove deforestation (Tinh et al., 2022). In the northwestern Puttalam district of Sri Lanka, shrimp pond expansion was responsible for 92% of the mangrove forest loss from 1973 to 2021 (Ofori et al., 2023). Furthermore, urban development and artificial planting also affected the changes in their dynamics. For instance, research indicates that the construction of the Dongzhai Harbor in Hainan Province, China, led to significant mangrove loss (Du et al., 2023). In Vietnam's Thanh Hoa and Nghe An Provinces, approximately 6318 ha of mangroves were planned to be artificially planted from the early 1990s to 2023 (Nguyen et al., 2021). Additionally, rising sea levels threaten mangrove survival (Feng et al., 2020; Zhang et al., 2023), and coastal erosion damages mangrove habitats (Jayanthi et al., 2022; Gitau et al., 2023), leading to mangrove loss (Phan and Stive, 2022). Moreover, typhoons, a significant factor in mangrove forest loss through high-energy winds accompanied by destructive waves and storm surges (Asbridge et al., 2018; Sippo et al., 2018; Simard et al., 2019), caused extensive mangrove die-off (Walcker et al., 2019). Thus, a weak hydrodynamic environment is more conducive to mangrove propagation (Long et al., 2022), during which time insufficient sediment transport by

currents imposes survival stress (Phan and Stive, 2022). Moreover, invasive alien species compete for habitat resources, which could also lead to mangrove degradation and loss (Gao et al., 2018; Wang et al., 2019a). However, previous studies have primarily focused on the causes of decline in mangrove areas to better understand long-term dynamic changes, with relatively scarce research on disturbances in recovery and expansion areas, especially in regions invaded by exotic species. Therefore, understanding the dynamic impacts of human activities and natural environmental stress factors on the recovery process of mangrove ecosystems through long-term studies holds significant theoretical and practical value for the protection of fragile mangrove ecosystems in recovery areas.

Overall, different natural environments and human activity intensities have different influences on the dynamic processes of mangrove restoration and expansion. Moreover, there are currently widespread invasions of *S. alterniflora* and rapid expansions of the exotic mangrove species *Sonneratia apetala* along tidal flats in China (Liu et al., 2018; Zhao et al., 2022), leading to scenarios in which local intertidal ecological environments are gradually dominated by biological invasions (Chen and Ma, 2015). Consequently, whether indigenous mangrove species can rapidly form dominant communities during their recovery and occupy space and resources is ecologically significant for resisting the large-scale spread and invasion of alien species. Thus, understanding the impact of regional environmental changes on the dynamics of mangrove recovery and expansion, especially in areas affected by invasive species, is valuable for monitoring and conserving vulnerable global mangrove ecosystems. Therefore, the Dandou Sea (DDS), an area within the Guangxi Shankou Mangrove National Nature Reserve in China where the invasive species *S. alterniflora* is rampant, was selected to examine the dynamic changes in mangrove forests. The objectives of this study were (i) to detect the changes in mangrove forests in the DDS from 1987 to 2021; (ii) to investigate the main factors affecting the dynamic changes in mangrove forests in the DDS; and (iii) to elucidate whether sea level rise could contribute to the loss of local mangrove forests. This work may provide a reference for understanding the loss and management of similar intertidal mangrove forests.

2 Data and methods

2.1 Study area

Located on the south-east coast of the Guangxi Province and situated on the west side of the Shatian Peninsula (Fig. 1), the DDS stretches from north-east to south-west,

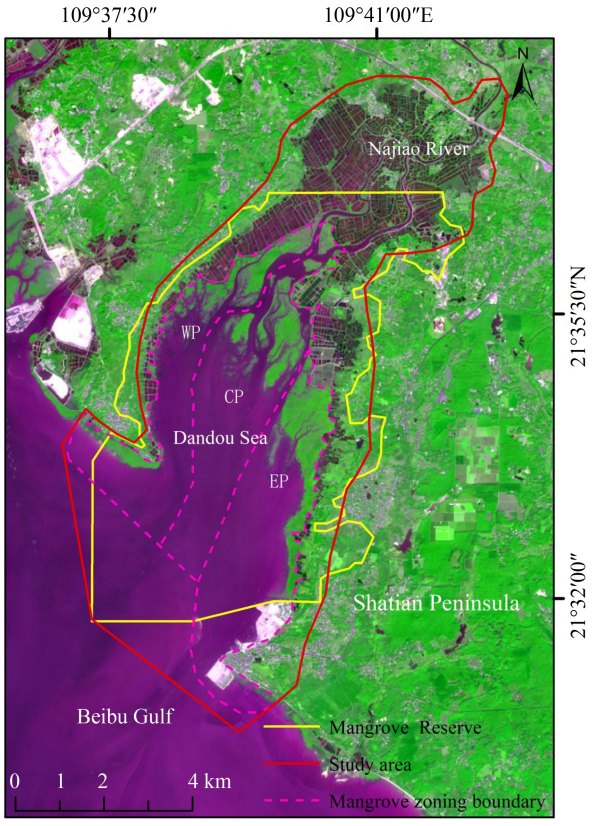

Fig. 1 Study area. The study area is in the Guangxi Shankou Mangrove National Nature Reserve which is located on the southeast coast of the Guangxi Province, with Dandou Sea situated within the reserve. The scope of the DDS study area, where the mangroves distribution area is divided into three parts: west part (WP), central part (CP), and east part (EP). The remote sensing imagery is sourced from the Sentinel-2A image dated December 13, 2021.

connecting the BBG to its south-west with a bay mouth width of 4.74 km. It is approximately 6.83 and 59.97 km away from the Tieshan Port tide gauge station and Beihai tide gauge station, respectively (Fig. 1). The Najiao River had flowed in from the northern region, depositing suspended sediments within the bay and forming extensive tidal flats. The tidal regime is classified as an irregular diurnal tide, with an average tidal range of 2.53 m and a maximum tidal range of about 6.25 m (Wang et al., 2014). Influenced by summer winds, waves propagate from the BBG into the bay mouth with an average height of 0.8 m. Conversely, winter wind-induced waves from the BBG have minimal impact (Qi et al., 2019). Located in the subtropical marine monsoon climate zone, the DDS has experienced hot and rainy summers, and mild and humid winters, with an average annual temperature of 23.8°C and an average annual precipitation of 1704 mm (Wang et al., 2019b).

The intertidal zone of the DDS provides a natural habitat for extensive mangrove proliferation. However, in the 1970s and 1980s, the mangroves have undergone

massive deforestation (Zhang et al., 2015). On September 30, 1990, the Guangxi Shankou Mangrove National Nature Reserve was established, divided into Yingluo Port and DDS areas. After a boundary survey in 2019, the reserve's coverage reached 8003 ha, with Yingluo Port and DDS areas spanning 2868.20 and 5134.80 ha, respectively (Fig. 1). From 1987 and 2021, the mangrove forests in the DDS have been in a state of restoration and expansion. During this process, they have been disturbed by external environmental factors, affecting the recovery and evolution of the mangroves, even their direction, inhibiting the comprehensive expansion of the mangrove area, and leading to a deterioration of the mangrove ecosystem. Particularly, since 1997, *S. alterniflora* have rapidly proliferated and expanded in the DDS, occupying vast bare tidal flats and some mangrove areas. Based on the geomorphological features, the DDS intertidal zone was further divided into the east part (EP), central part (CP), and west part (WP) in this study (Fig. 1).

2.2 Data source

Based on the GEE cloud platform, the multispectral remote sensing images from Landsat 5 TM and Landsat 8 OLI from 1987 to 2021 were retrieved and the land cover information of the DDS was extracted. The bare tidal flats were extracted based on the multispectral remote sensing images, captured during low tide from 1992 and 2021, which were obtained from the United States Geological Survey(Table 1). The historical tidal data for Tieshan Port and Beihai tide gauge stations were sourced from the Dayu Tide Chart and the South China Sea Branch of the State Oceanic Administration, and the average sea level data for Beihai from 1980 to 2021 were derived from the South China Sea Branch of the State Oceanic Administration and the 2021 China Sea Level Bulletin.

2.3 Methods

2.3.1 Land cover extraction and shoreline analysis

This study utilized the GEE cloud platform to retrieve multispectral remote sensing data from Landsat 5 TM and Landsat 8 OLI for the study area from 1987 and 2021. Based on the original spectral bands, calculate four spectral indices (Table 2). The study area was divided into eight categories: water, aquaculture ponds, mangrove forests, construction land and bare land, woodland, cultivated land, bare tidal flats, and *S. alterniflora*. The random forest supervised learning algorithm was employed for classification, with both overall accuracy and kappa accuracy exceeding 87%. Additionally, using the ENVI software and the support vector machine classifier, bare flats were extracted from the 1992 and 2021 Landsat 5 TM and Landsat 8 OLI multispectral remote sensing images. The digital shoreline analysis system extension tool in ArcGIS was then used to calculate the expansion and erosion rates of the DDS bare flat shoreline from 1992 to 2021. The transects were spaced 100 m apart, 187 transects in total, and numbered clockwise from west to east. The numbering ranges for the WP, CP, and EP areas of the DDS were 1–76, 77–97, and 98–187, respectively (Fig. 2(a)). Similarly, the change rates of the DDS mangroves from 1992 to 2021 were calculated, with transect numbers for the WP, CP, and EP areas being 1–63, 64–80, and 81–148, respectively (Fig. 2(b)).

2.3.2 Centroid migration

The centroid accurately represented the spatial distribution of mangroves and *S. alterniflora*. By comparing the changes in centroids between different years, the dynamic spatial changes in mangroves and *S.*

Table 1 Landsat satellite remote sensing image information and tidal level at acquisition time

Imaging acquisition time	Remote sensing satellite	Data ID	Spatial resolution /m	Tidal level at the time of imaging /m
July 12, 1992	Landsat 5 TM	LT51240451992194BJC01	30	130
July 12, 2021	Landsat 8 OLI	LC81240452021193LGN00	30	147

Table 2 Spectral index for classification

Index name	Computational formula	Reference literature
Modified normalized difference water index(MNDWI)	$\mathrm{MNDWI}=\frac{(\rho_{\mathrm{green}}-\rho_{\mathrm{swir}})}{(\rho_{\mathrm{green}}+\rho_{\mathrm{swir}})}$	Xu (2005)
Normalized difference built-up index (NDBI)	$\mathrm{NDBI}=\frac{(\rho_{\mathrm{swir}}-\rho_{\mathrm{nir}})}{(\rho_{\mathrm{swir}}+\rho_{\mathrm{nir}})}$	Zha et al. (2003)
Normalized difference vegetation index(NDVI)	$\mathrm{NDVI}=\frac{(\rho_{\mathrm{nir}}-\rho_{\mathrm{red}})}{(\rho_{\mathrm{nir}}+\rho_{\mathrm{red}})}$	Rouse et al. (1974)
Mangrove vegetation index(MVI)	$\mathrm{MVI}=\frac{(\rho_{\mathrm{nir}}-\rho_{\mathrm{green}})}{(\rho_{\mathrm{swir}}-\rho_{\mathrm{green}})}$	Baloloy et al. (2020)

Note: ρ_{green}, ρ_{red}, ρ_{swir}, ρ_{nir} correspond to the green, red, shortwave infrared, and near-infrared bands in Landsat imagery, respectively.

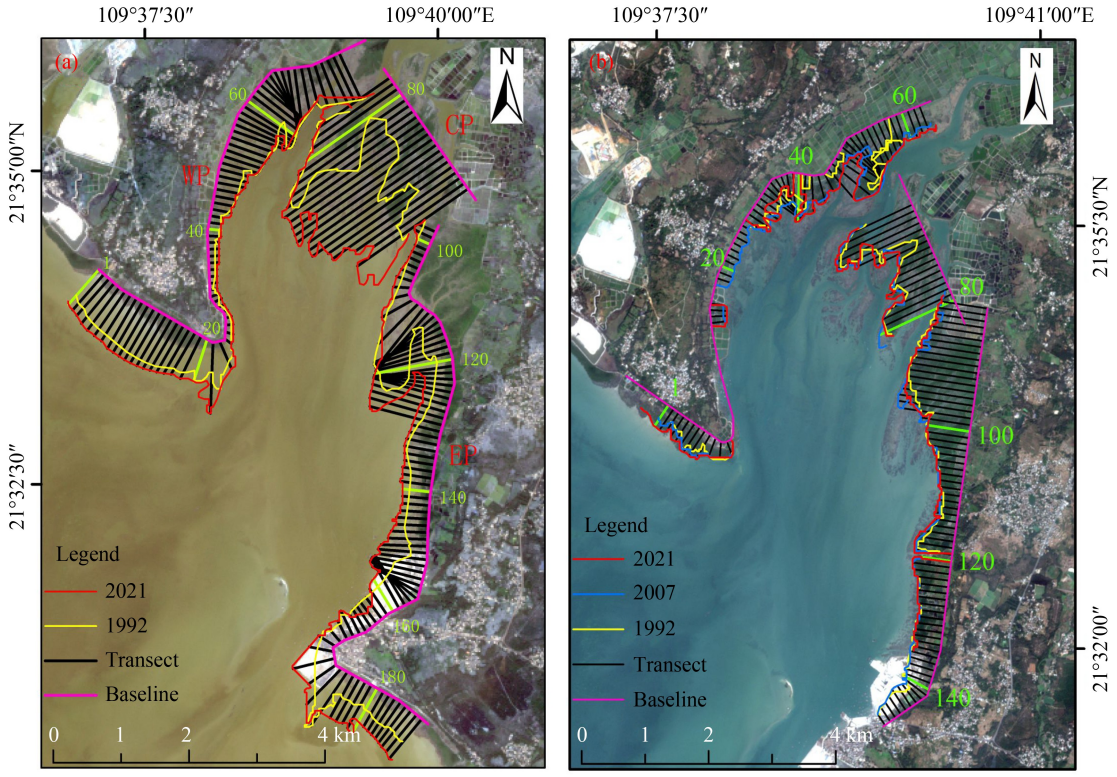

Fig. 2 Transects of the mangrove forest shoreline and mudflat shoreline in the DDS from 1992 to 2021, (a) transects of the mudflat shoreline; (b) transects of the mangrove shoreline.

alterniflora were quantified (Lu et al., 2018). ArcGIS software was used to separately calculate the centroids of mangroves and *S. alterniflora* in the DDS, and the centroid calculation formulas were as follows (Jia et al., 2015):

$$X_t = \sum_{i=1}^{n} C_{ti}X_{ti} \Big/ \sum_{i=1}^{n} C_{ti}, \quad (1)$$

$$Y_t = \sum_{i=1}^{n} C_{ti}Y_{ti} \Big/ \sum_{i=1}^{n} C_{ti}, \quad (2)$$

where X_t and Y_t represent the latitude and longitude coordinates of the centroid in year t; C_{ti} represents the area of the ith patch in year t; X_{ti} and Y_{ti} represent the latitude and longitude coordinates of the ith patch in year t; and n represents the number of patches in year t.

To visually express the spatial movement of the DDS mangrove centroids from 1987 to 2021, the centroids for the years 1987, 1992, 1997, 2002, 2007, 2013, 2017, and 2021 were calculated separately. Distances between centroids for each period were computed, and a trajectory map of the mangrove centroids was plotted. Similarly, centroids for *S. alterniflora* in DDS for the years 1997, 2002, 2007, 2013, 2017, and 2021 were calculated, distances between centroids for each period were determined, and a trajectory map of the *S. alterniflora* centroids was created.

2.3.3 Calculation of land use type transitions

The ArcGIS software possesses robust spatial analysis capabilities. Its overlay analysis tools, specifically the Erase and Intersect functions, are adept at analyzing spatial land class transitions. The fundamental approach involved using the Erase function on two vector data sets of the same land class from different years to calculate spatial expansion or loss. Subsequently, the results were intersected with other land classes using the Intersect function. This process determines the encroachment of other land classes on the given class or how the given land class has expanded into others (Mou et al., 2012). Based on these operations, the periods 1987–1992, 1992–1997, 1997–2002, 2002–2007, 2007–2013, 2013–2017, and 2017–2021 were analyzed to statistically determine the area of other land classes encroaching on mangroves and the area where mangroves expanded into other land classes. Similarly, for the period 1987–2021, calculations were made for aquaculture ponds encroaching on woodland, cultivated land, construction land and bare land, mangroves, bare tidal flats, and *S. alterniflora*.

2.3.4 Calculation of landscape pattern indices

The landscape pattern index is useful for evaluating the quality and status of mangrove ecosystems (Xiong et al., 2024). Identifying the long-term changes in this index is

crucial for monitoring the health of mangrove ecosystems as it effectively reflects their resilience to external environmental disturbances. Consequently, this study employed Fragstats software to calculate the mangrove forest landscape pattern from 1987 to 2021: 1) The patch density (PD) measures the degree of landscape fragmentation. 2) The patch cohesion index (COHESION) characterizes the degree of connectivity within the mangrove patch structure. 3) The splitting index (SPLIT) measures the degree of isolation of the mangrove landscape. 4) The landscape shape index (LSI) characterizes the conditions influenced by external environmental factors. The computational formulas were based on McGarigal and Marks (1995):

$$\mathrm{PD} = \frac{\mathrm{NP}}{\mathrm{A}}, \tag{3}$$

$$\mathrm{COHESION} = \left[1 - \frac{\sum_{i=1}^{m}\sum_{j=1}^{n} P_{ij}}{\sum_{i=1}^{m}\sum_{j=1}^{n} P_{P_{ij}}\sqrt{a_{ij}}}\right]\left[1 - \frac{1}{\sqrt{A}}\right]^{-1} \times 100, \tag{4}$$

$$\mathrm{SPLIT} = \frac{A}{2A_i}\sqrt{\frac{n_i}{A}}, \tag{5}$$

$$\mathrm{LSI} = \frac{0.25E}{\sqrt{A}}. \tag{6}$$

3 Results

3.1 Changes in mangrove forest areas

From 1987 to 2021, the mangrove forest area in the DDS exhibited a growth trend, increasing from 225.90 ha in 1987 to 451.76 ha in 2021 and undergoing three distinct phases of change. Specifically, between 1987 and 1996, the mangrove area expanded rapidly from 225.90 to 362.93 ha, with a growth rate of 16.77 ha/yr. From 1997 to 2011, the growth rate decelerated, as the mangrove area expanded from 365.09 to 432.19 ha, with a mean rate of 6.61 ha/yr. However, between 2013 and 2021, the mangrove forest area stagnated (Fig. 3).

Between 1987 and 2021, the mangrove area of the DDS exhibited an overall increasing trend in different regions. Specifically, the mangrove areas in the WP and CP underwent three phases of change. In the WP, from 1987 to 1996, the mangrove area grew rapidly, increasing from 4.00 to 80.50 ha, with a growth rate of 8.90 ha/yr. From 1997 to 2011, the growth rate slowed, with the mangrove area increasing from 81.59 to 104.48 ha, with a growth rate of 2.55 ha/yr. From 2013 to 2021, the change trend was not significant (Fig. 4(a)). In the CP, from 1987 to 1996, the mangrove area grew rapidly, increasing from 29.39 to 71.35 ha, with a growth rate of 3.40 ha/yr. From 1997 to 2011, the growth rate slowed, with the area of mangroves expanding from 67.18 to 119.80 ha, with a growth rate of 2.68 ha/yr. From 2013 to 2021, the change trend was not significant (Fig. 4(b)). In the EP, from 1987 to 2021, the mangrove area increased slowly, with a growth rate of 0.83 ha/yr (Fig. 4(c)).

3.2 Spatial distribution of mangrove forests

From 1987 to 2021, the mangroves in the WP, CP, and

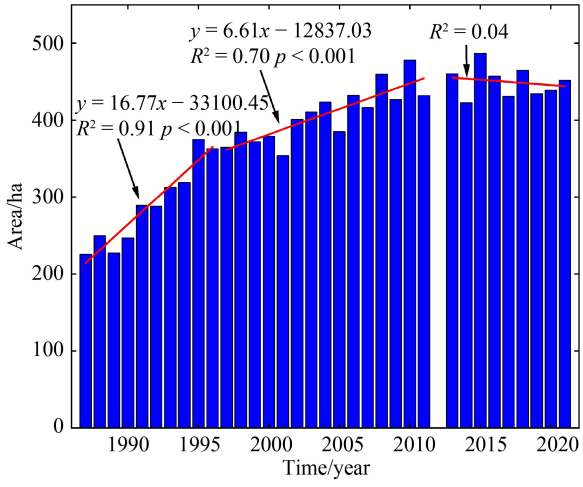

Fig. 3 Changes in mangrove forest areas in the DDS from 1987 to 2021.

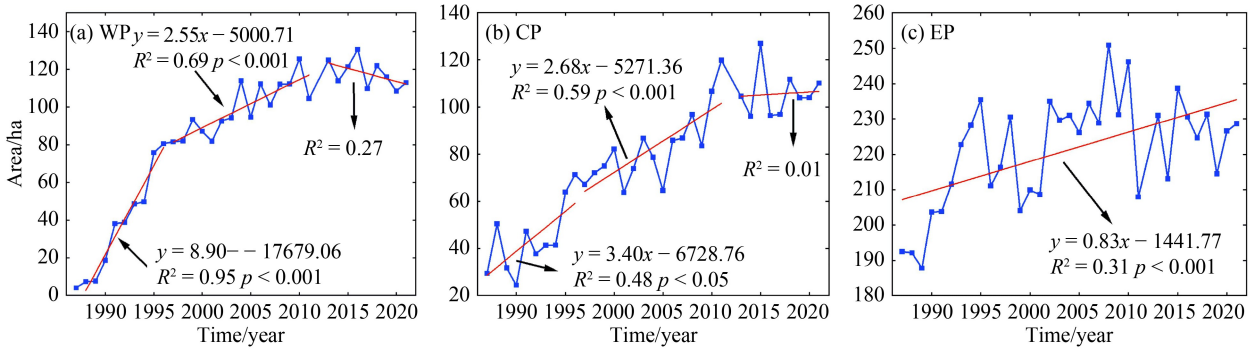

Fig. 4 Changes of mangrove forest areas in various regions of the DDS from 1987 to 2021, (a) the west part; (b) the cent part; (c) the east part.

EP of the DDS underwent different spatial changes (Fig. 5). In the WP of the DDS in 1987, large areas of intertidal zones were exposed as bare flats, with only approximately 4.00 ha of scattered mangroves on the tidal flats (Fig. 5(a)). After 1987, mangroves in the WP tidal flats began to expand extensively. By 1992, 38.88 ha of mangroves had settled on the tidal flats, primarily distributed in the southern and northern coastal tidal flats, covering areas of 17.32 ha and 21.56 ha, respectively (Fig. 5(b)). From 1992 to 2002, the expansion of mangrove patches in the southern coastal intertidal zone was not significant. In contrast, the northern mangrove patches expanded rapidly, merging into three major mangrove patches. Moreover, mangrove patches appeared in the middle coastal tidal flats and expanded slowly (Figs. 5(b)–5(d)). However, from 2007 to 2021, the mangrove patches tended to fragment, with the most severe fragmentation occurring in the areas where the middle and northern coastal tidal flats adjoin (Figs. 5(e)–5(h)).

The spatial pattern of mangroves in the CP of the DDS was similar to that in the WP, and it also underwent significant changes from 1987 to 2021. In 1987, the intertidal zone of the CP was largely bare, with only 29.39 ha of mangroves scattered in the southern tidal flats (Fig. 5(a)). From 1987 to 1992, the mangroves further expanded in the southern tidal flats, and patches of mangroves also appeared in the northern end (Fig. 5(b)). By 1997, there was an overall expansion of the original patches, which were still predominantly distributed in the southern tidal flats and increased to 67.18 ha, while *S. alterniflora* began to reproduce in the southern tidal flats (Fig. 5(c)). From 2002 to 2013, the mangroves remained concentrated in the southern tidal flats and expanded slowly, with other tidal flats sparsely populated with mangroves (Figs. 5(d)–5(f)). In contrast, from 2013 to 2021, there was no significant spatial expansion of mangroves (Figs. 5(f)–5(h)).

The spatial pattern of mangroves in the EP of the DDS differed from that of the WP and CP, with a relatively stable change process from 1987 to 2021. In 1987, 192.51 ha of mangroves were concentrated and continuously distributed along the EP coastal tidal flats, accounting for 85.22% of the total mangrove area in the DDS during the same period (Fig. 5(a)). From 1987 to 1992, the mangroves expanded toward the southern and northern

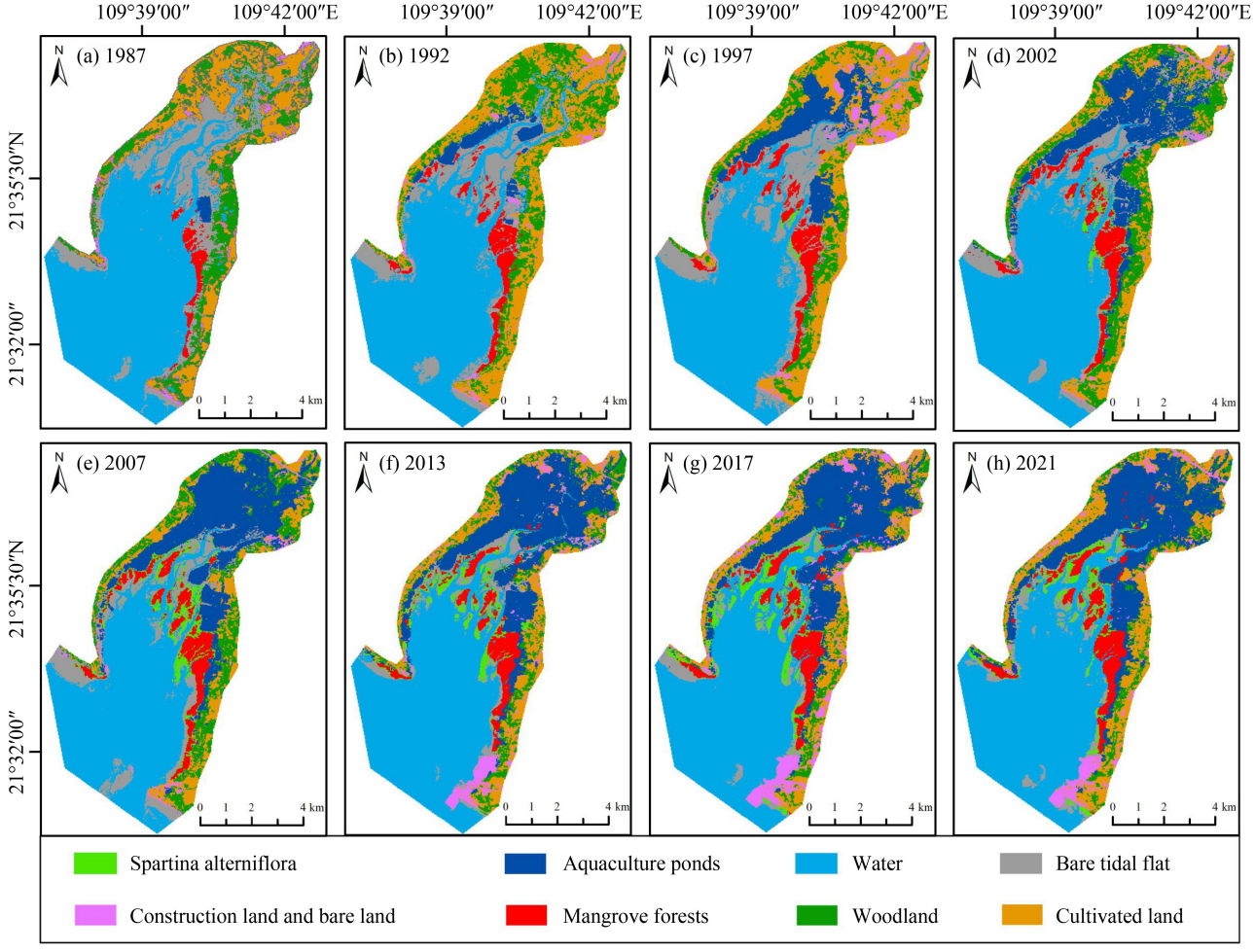

Fig. 5 Spatial dynamics changes of mangrove forests in the DDS from 1987 to 2021.

tidal flats (Fig. 5(b)). During the subsequent period from 1997 to 2007, the mangrove area remained stable (Figs. 5(c)–5(e)). However, between 2007 and 2013, there was a loss of approximately 19.99 ha of mangroves in the southern tidal flats (Figs. 5(e)–5(f)). Moreover, from 2013 to 2021, the mangrove area remained relatively stable (Figs. 5(f)–5(h)).

3.3 Landscape pattern in mangrove forests

From 1987 to 1996, the patch density of mangroves in the DDS increased from 0.77 to 0.86 n/ha. The patch cohesion index decreased from 96.16% to 95.63%, the splitting index decreased from 1586.76% to 1271.41%, and the landscape shape index increased from 7.89% to 9.60%. The results indicated that during this period, the expansion of the mangrove area was mainly based on the generation of new patches on the existing ones. The newly formed mangrove patches were not yet fully developed and contained a large number of forest windows. With the increase in new patches, the internal structural connection of the mangrove patches in the DDS decreased, the connection between patches strengthened, and the shape of the patches became more complex, which led to their decreasing ability to resist external disturbances (Fig. 6). From 1997 to 2011, the mangrove landscape exhibited deterioration. The patch density of mangroves increased from 0.60 to 1.40 n/ha, an increase of 2.33 times compared to that in the previous period. Additionally, the patch cohesion index decreased from 95.79% to 95.14%, the splitting index decreased from 1258.00% to 1015.35%, and the landscape shape index increased from 9.13% to 10.69% (Fig. 6). From 2013 to 2021, the patch density of mangroves decreased from 1.50 to 1.18 n/ha, the patch cohesion index increased from 94.72% to 95.35%, the splitting index increased from 791.38% to 824.43%, and the landscape shape index increased from 9.30% to 9.37%. The mangrove landscape improved compared to that in the previous period.

4 Discussion

4.1 Impact of land use conversion

Human activities such as logging, converting coastal areas into farmland, enclosing ponds for aquaculture, and

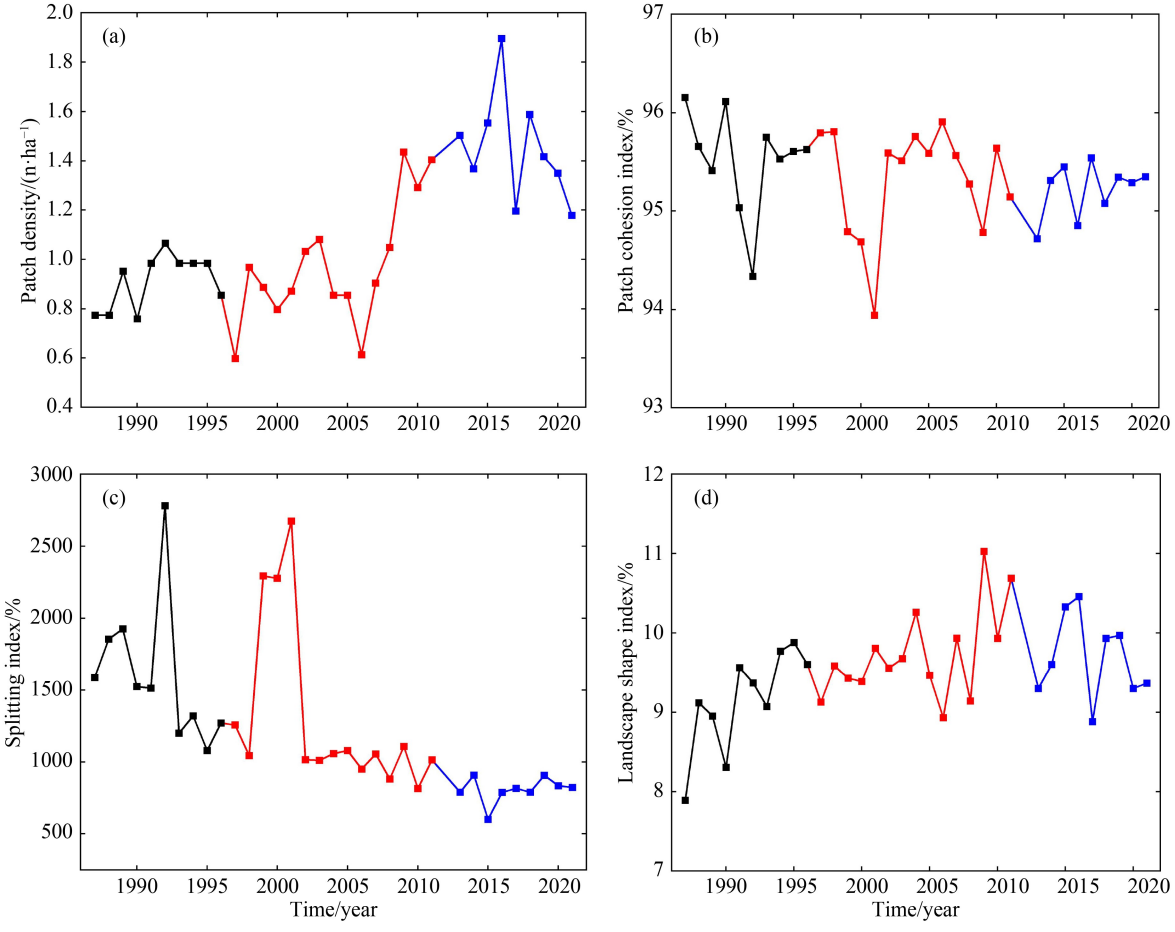

Fig. 6 Landscape pattern index changes of mangrove forests in the DDS, (a—d) the black, red, and blue lines correspond to the years 1987 to 1996, 1997 to 2011, and 2013 to 2021, respectively.

filling seas to create land directly resulted in the loss of mangrove forests (Duke et al., 2007; Bunting et al., 2022; Tinh et al., 2022). From 1987 to 2021, in the DDS, the cumulative encroachment of mangroves by farmland, forestland, aquaculture ponds, and *S. alterniflora* was 8.65, 13.99, 25.47, and 112.38 ha, respectively, contributing 3.21%, 5.19%, 9.45%, and 41.69%, respectively, to the loss of mangroves (Table 3). Concurrently, construction land and bare land accounted for a loss of 21.32 ha of mangroves and contributed 7.91% of the overall mangrove loss (Table 3). Additionally, economic activities such as people gathering seafood on bare flats during ebb tides and large oyster farming (Fig. 7) have caused damage to both mangrove saplings and mature forests, leading to the degradation of local mangrove areas into bare flats (He et al., 2012). It was estimated that between 1987 and 2021, a total of 87.75 ha of mangroves in the DDS degraded into bare flats, contributing 32.55% to the loss of mangroves (Table 3). These human activities, to some extent, led to an increase in the number of mangrove patches, a decrease in the cohesion index, and an increase in the landscape shape index (Fig. 6), which resulted in a deterioration of the mangrove landscape.

From 1987 to 2021, the expansion of mangroves in the DDS primarily encroached upon bare tidal flats, with a cumulative encroachment of 392.91 ha, accounting for 68.75% of the total mangrove expansion area (Table 4). However, aquaculture ponds encroached upon 641.80 ha of bare tidal flats suitable for mangrove growth between 1987 and 2021 (Table 5 and Fig. 5), limiting the spatial expansion of mangroves. Compared to other mangrove distribution areas where aquaculture ponds directly encroached on mangroves, contributing to a greater

Table 3 Modes of mangrove forest occupation in the DDS region from 1987 to 2021 during different periods

Time/year	Woodland /ha	Cultivated land/ha	Construction land and bare land/ha	Aquaculture ponds/ha	*S. Alterniflora* T. /ha	Bare tidal flat/ha	Total/ha
1987—1992	2.00	0.08	0.00	0.00	0.00	1.33	3.41
1992—1997	5.00	0.17	0.00	1.92	1.08	32.87	41.04
1997—2002	0.92	0.00	0.00	4.57	11.57	12.82	29.88
2002—2007	0.08	1.83	0.00	1.50	40.21	3.33	46.95
2007—2013	0.75	0.33	19.99	4.41	39.79	30.48	95.75
2013—2017	2.66	1.08	0.75	5.33	9.07	3.84	22.73
2017—2021	2.58	5.16	0.58	7.74	10.66	3.08	29.80

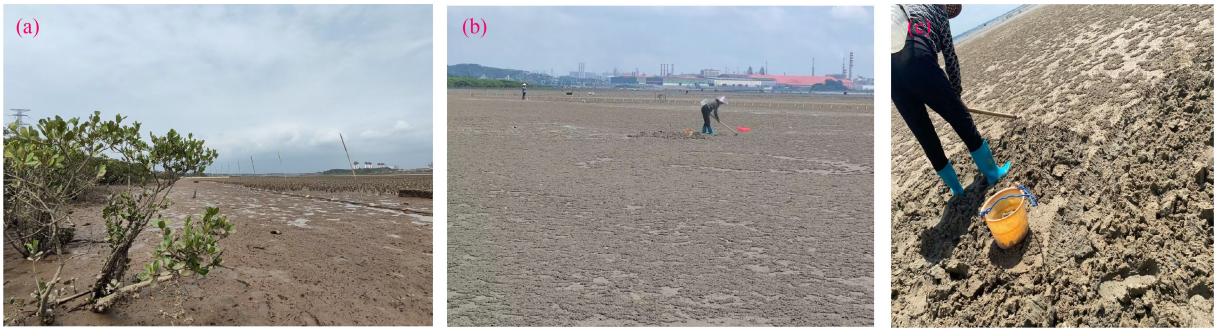

Fig. 7 Human activities causing damage to mangrove forests and tidal flats, (a) large-scale oyster farming, (b and c) people gather seafood on the tidal flats during ebb tide.

Table 4 Mangrove forests encroached by other land types from 1987 to 2021 in the DDS

Time/year	Woodland/ha	Cultivated land/ha	Construction land and bare land/ha	Aquaculture ponds/ha	*S. Alterniflora* /ha	Bare tidal flat/ha	Total/ha
1987—1992	1.00	0.08	0.00	0.58	0.00	181.51	183.17
1992—1997	4.32	0.00	0.00	0.75	0.00	77.51	82.58
1997—2002	3.33	0.00	0.00	0.17	4.41	59.28	67.19
2002—2007	3.33	0.00	0.00	1.08	27.47	26.90	58.78
2007—2013	1.00	1.25	0.00	3.00	32.55	17.48	55.28
2013—2017	6.74	1.75	0.00	9.66	33.55	19.82	71.52
2017—2021	4.58	1.33	0.25	8.91	27.47	10.41	52.95

Table 5 Area of various land types and encroachment of aquaculture ponds in the DDS in 2021 and 1987

	Woodland/ha	Cultivated land/ha	Construction land and bare land/ha	Mangrove forests/ha	Bare tidal flat/ha
1987	764.14	1510.33	112.88	225.90	-
2021	396.44	923.49	257.95	451.76	-
Encroachment of aquaculture ponds	219.42	684.50	43.70	3.41	641.80

proportion of mangrove loss (Tinh et al., 2022; Ofori et al., 2023), the aquaculture ponds in the DDS mainly encroached on large areas of bare tidal flats suitable for mangrove growth, inhibiting mangrove recovery and expansion. Therefore, in the process of mangrove restoration and protection, monitoring of the dynamic changes in bare tidal flats in the intertidal zone should be strengthened to avoid large-scale losses and pressure on the recovery and expansion space of mangroves.

4.2 Impact of large-scale construction of aquaculture ponds

Tidal hydrodynamics influenced the spatial expansion of mangroves. Mudflats with weaker hydrodynamics were more conducive to the growth of seedlings, thereby promoting the rapid expansion of mangrove communities (Abdul Azeez et al., 2022; Long et al., 2022). Conversely, in estuaries and coastal tidal flats with strong hydrodynamics, mangrove seedlings struggled to establish, the expansion of mangrove communities was notably inhibited (Le Minor et al., 2019), and mature mangrove communities also suffered from erosion losses (Tinh et al., 2022). Severe tidal hydrodynamics-induced coastal erosion led to an average loss of more than 400 ha/yr of mangroves in the Mekong Delta of Vietnam from 1973 to 2020 (Phan and Stive, 2022). In this study, from 1987 to 2021, the area of aquaculture ponds in the DDS increased from 43.13 to 1635.96 ha (Fig. 8(a)). This increased encroachment on woodland, construction land and bare land, and cultivated land by 219.42, 43.70, and 684.50 ha, respectively (Table 5), leading to an increase in tidal prism, tidal flow, and enhanced hydrodynamics (Yang et al., 2020). Remote sensing technology revealed severe erosion in the Najiao River estuary from 1992 to 2021 (Figs. 8(b) and 8(c)), confirming that regional hydrodynamics strengthened. This weakens the resistance of mangrove seedlings to tidal hydrodynamics and causes erosion along localized transects of the mangrove shoreline, thereby damaging the habitat (Fig. 9).

Moreover, analysis of the shorelines of mangrove forests in the DDS from 1992 to 2021 revealed that the overall rate of mangrove expansion in the DDS was approximately 2.94 m/yr seaward (Fig. 9). Specifically, in the WP, CP, and EP of the DDS, the rates of mangrove expansion toward the sea were 4.81, 3.06, and 1.17 m/yr, respectively. Additionally, in transect 32 in the WP and transects 84 and 140 in the EP, mangroves were retreating at rates of −6.05, −3.21, and −4.21 m/yr, respectively (Fig. 9). It was evident that the intensified hydrodynamics led to localized erosion and the retreat of mangrove intertidal areas. Similar localized erosion of mangroves intertidal areas was observed in the northern flow of the BBG, the Nanliu River, and the Qinzhou River estuaries (Fig. 10). However, in most parts of the DDS, the impact of intertidal erosion on the mangrove fringe was relatively minor.

4.3 Impact of the invasive species *Spartina alterniflora*

S. alterniflora, an invasive species in China (Liu et al., 2018), possesses strong environmental adaptability and reproductive capacity (Pan et al., 2016). *S. alterniflora* has damaged the biodiversity of China's coastal zones, especially mangrove ecosystems (Gao et al., 2018; Wang et al., 2019a). Since *S. alterniflora* was introduced to the

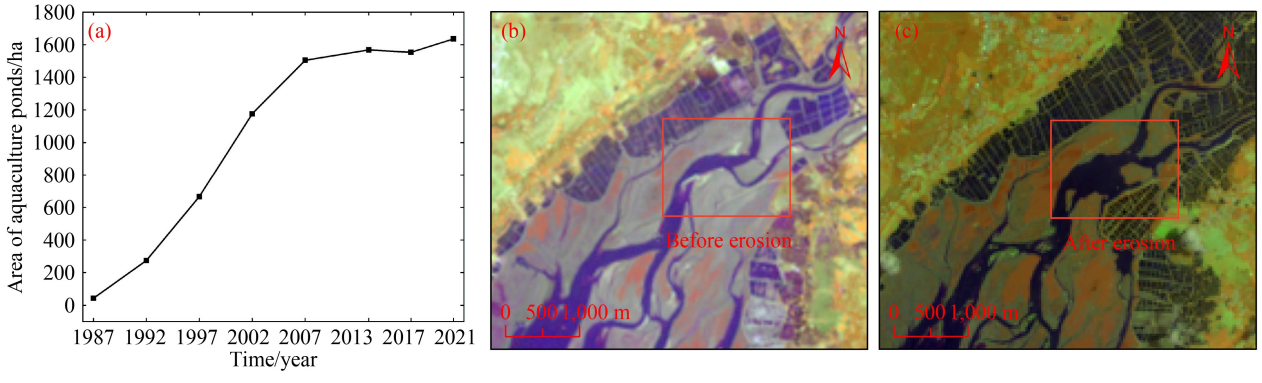

Fig. 8 Changes in the area of aquaculture ponds and regional topography in the DDS from 1987 to 2021, (a) changes in pond area from 1987 to 2021; (b) before erosion on July 12, 1992, with a tidal level of 130 cm; (c) after erosion on July 12, 2021, with a tidal level of 147 cm.

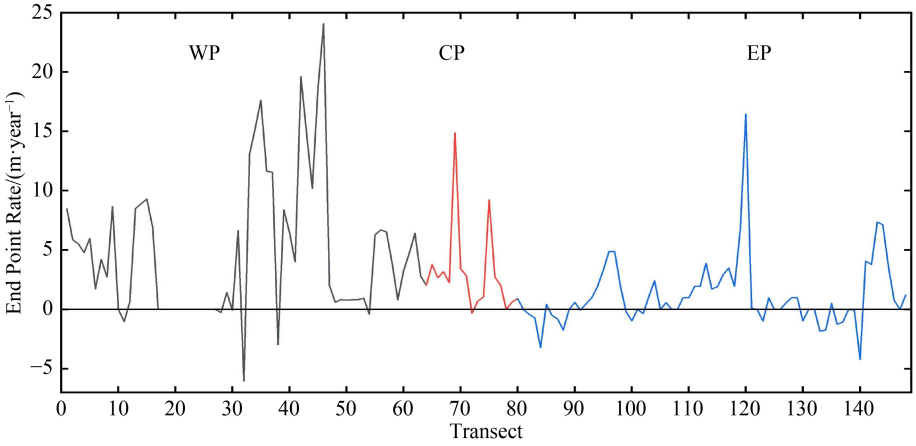

Fig. 9 Endpoint rate of the mangrove forests shoreline in the DDS from 1992 to 2021.

Fig. 10 Erosion and degradation of mangrove forest tidal flats, (a) vertical erosion and degradation of mangrove tidal flats in Nanliujiang estuary; (b) erosion and degradation of mangrove forest tidal flats in Qinjiang estuary; (c) mangrove forests collapses and dies in Qinjiang estuary.

DDS in 1979 (Pan et al., 2016), it has undergone four phases: introduction, establishment, spread, and outbreak. From 1987 to 1996, the *S. alterniflora* population in the DDS was in the establishment phase, and it had no impact on the expansion of mangroves (Fig. 11(a)). As a result, the mangrove area in the DDS increased at a rate of 16.96 ha/yr (Fig. 3), and those in the WP and CP increased at rates of 8.90 and 3.40 ha/yr, respectively (Figs. 4(a) and 4(b)). While mangrove patch connectivity increased during this time, overall resistance to external disturbances decreased (Fig. 6). Consequently, from 1997 to 2011, during the spread and outbreak phases of *S. alterniflora*, its area increased to 419.52 ha, closely bordering and locally invading mangrove patches (Fig. 5), leading to a slowdown in mangrove expansion (Figs. 3 and 11(a)) and a deterioration of the mangrove landscape (Fig. 6). Consequently, the growth rate of mangroves in the DDS during this period decreased to 6.61 ha/yr (Fig. 3), with growth rates in the WP and CP decreasing to 2.55 and 2.68 ha/yr, respectively (Figs. 4(a) and 4(b)). From 2013 to 2021, the area of *S. alterniflora* decreased to 343.59 ha (Fig. 11(a)) in response to anthropogenic control measures such as mowing and uprooting (Shen et al., 2022), and its invasion into mangroves significantly decreased (Table 3). The mangrove landscape showed signs of improvement (Fig. 6), but the restoration of the mangrove ecosystem remains urgent.

From 1997 to 2021, the centroids of mangroves and *S. alterniflora* in the DDS exhibited a high degree of consistency in spatial expansion, and both areas migrated northward (Fig. 11(b)). Moreover, from 1997 to 2021, changes in the centroid of mangroves and *S. alterniflora* showed a significant correlation with latitude, with $P = 0.011$ (Table 6). They highly overlapped spatially, hindering the expansion of mangroves. Additionally, *S. alterniflora* rapidly invaded mangrove patches along tidal channels or sparse areas of mangroves due to its efficient productivity (Jiang et al., 2022), leading to the fragmentation and degradation of mangrove patches (Fig. 12). Previous research has shown that the expansion of mangrove areas often results from the encroachment of construction lands, aquaculture ponds, and farmlands, contributing significantly to the loss of mangrove cover (Long et al., 2021; Du et al., 2023). In the case of the DDS, the invasion of *S. alterniflora* into mangrove areas was the most significant contributor to this loss, showing unique regional characteristics. The exploration of the long-term dynamic changes in the mangroves of the DDS due to *S. alterniflora* is vital for providing theoretical and practical references for addressing the invasion of alien

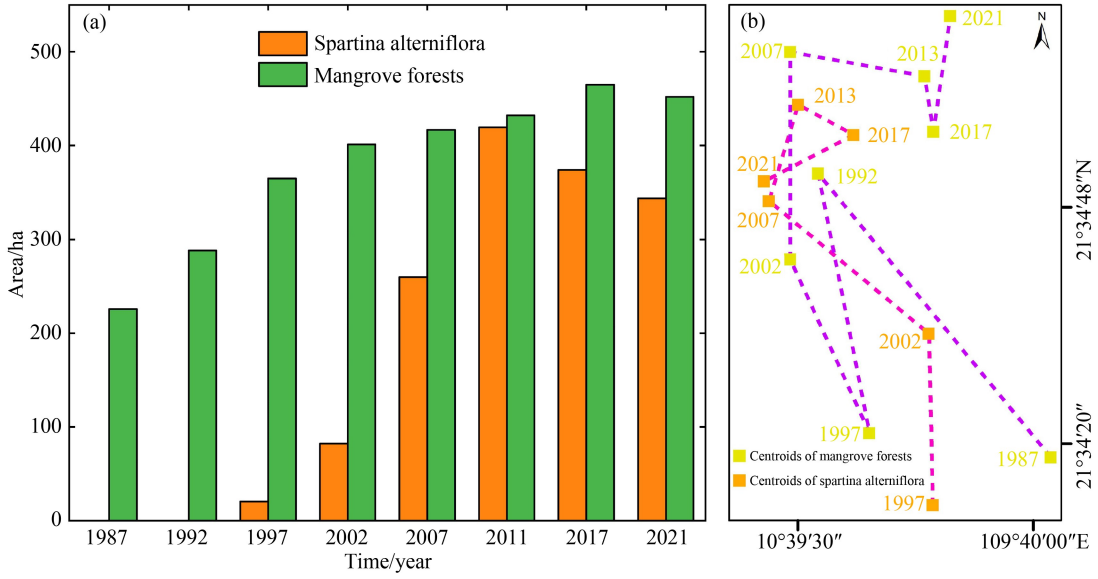

Fig. 11 Area and centroid changes of *Spartina alterniflora* and mangrove forests in the DDS, (a) Trends in the change of area between *Spartina alterniflora* and mangroves, (b) Trajectories of centroid changes between *Spartina alterniflora* and mangroves.

Table 6 Correlation analysis of the centroid latitude and longitude of mangroves and *Spartina alterniflora* in the DDS from 1997 to 2021

Name	Pearson correlation	Significance
Longitude	−0.315	$P = 0.542$
Latitude	0.914	$P = 0.011$

species in mangrove ecosystems. Additionally, for the control of *S. alterniflora* in the DDS region, it is recommended to prioritize the treatment of areas with sparse mangrove tree and sapling distributions, manage the bare tidal flats without mangroves, and disrupt the densely populated areas of *S. alterniflora* to address the challenges of mangrove fragmentation.

4.4 Impact of climatic factors

The increase in sea level caused by climate change was identified as a primary natural factor threatening the survival of mangrove forests (Feng et al., 2020; Zhang et al., 2023). At the same time, a moderate increase in temperature could, to some extent, promote the growth and development of plants. Studies have indicated that from 2000 to 2020, the annual average temperature in the prefectural city region where the Shankou Mangrove Reserve is located showed an increasing trend, and this trend was positively correlated with changes in the mangrove forest area (Shi et al., 2023). Moreover, a rise in temperature could lead to changes in the regional sea level. From 1980 to 2021, the average sea level in the Beihai increased by 0.188 cm per year (Fig. 13). Previous studies have indicated that the deposition rate of tidal flats in DDS mangrove areas was lower than the sea level rise rate. Coupled with the restriction imposed by concrete seawalls preventing their expansion inland, global sea level rise will inhibit the seaward expansion of

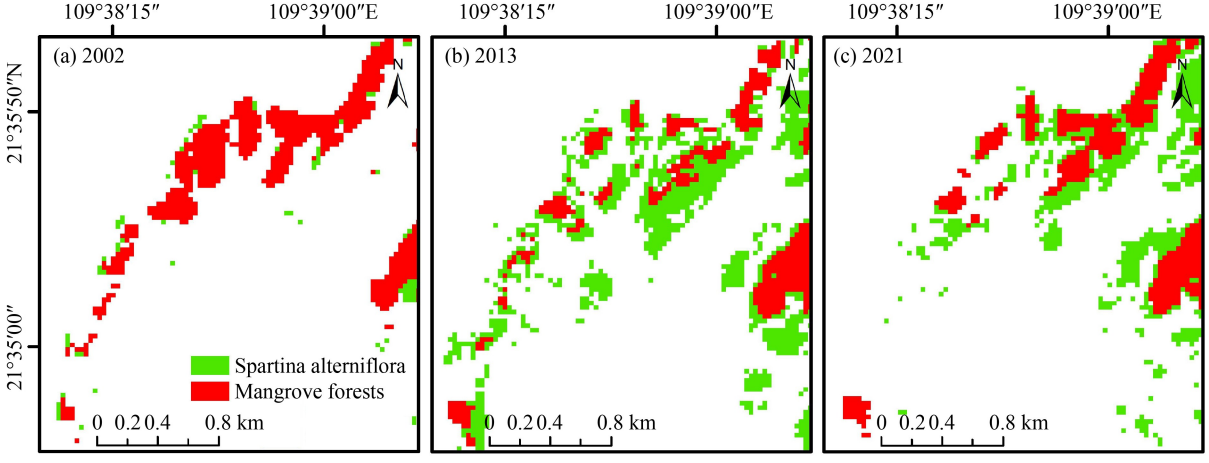

Fig. 12 Invasion of *Spartina alterniflora* leads to the fragmentation and degradation of mangroves in localized areas.

mangroves and result in losses (Xia et al., 2015; Lovelock et al., 2017). However, mangroves counteract sea level rise by expanding inland (Krauss et al., 2011; López‐Medellín et al., 2011). Although large-scale concrete seawalls distributed along the rear edge of mangrove tidal flats in China always limit the inland expansion of mangroves (Yue et al., 2023), intertidal mangrove tidal flats are capable of capturing suspended sediments from rivers and tides, leading to deposition in tidal flats. When the deposition rate surpasses the sea level rise rate, mudflats can continuously expand seaward and create space for mangroves (Kirwan and Megonigal, 2013; Yoshikai et al., 2022).

Analysis of the evolution of the bare tidal flat shoreline in the DDS from 1992 to 2021 revealed that it expanded seaward at a rate of 6.23 m/yr. The bare tidal flat shorelines in the WP, CP, and EP all expanded seaward, with expansion rates of 1.38, 29.21, and 4.96 m/yr, respectively (Fig. 14). Therefore, from 1992 to 2021, the overall shoreline of the DDS bare tidal flat advanced seaward, and regional sea level rise did not directly induce the retreatment of the mangrove forest in the DDS.

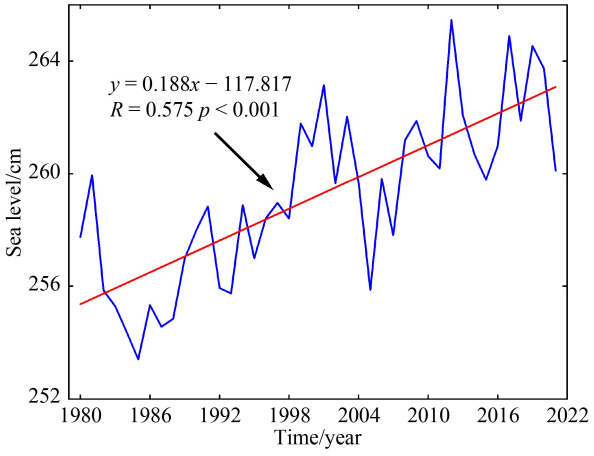

Fig. 13 The mean sea level changes at Beihai station from 1980 to 2021.

These results are consistent with those of Long et al. (2022), who reported that bare tidal flats in the delta of the Nanliu River in the northern part of the BBG in China were rapidly expanding. However, mangroves in the Mekong Delta are facing threats from rising sea levels (Phan and Stive, 2022), which might be due to differences in regional sea level rise rates and variations in sediment discharge into the sea. Changes in sea levels under the backdrop of global climate change still pose potential risks to mangroves in the DDS area.

Additionally, the coastal areas of the northern BBG are prone to tropical cyclone disasters during the summer and autumn seasons. From 1949 to 2013, the number of tropical cyclones affecting this region showed an increasing trend, with more than five cyclones occurring in 1994, 1995, 2011, 2012, and 2013 and reaching ten in 2013 (Li et al., 2014). The passage of tropical cyclones can cause extensive defoliation, branch breaking, and even death of mangroves (Walcker et al., 2019), such as the severe damage caused to the mangroves of Samar Province in the Philippines by the super typhoon "Haiyan" in 2013 (Long et al., 2016). Consequently, the expansion speed of the Nanliu River estuary mangroves was relatively faster in years with a lower frequency of typhoons and higher annual minimum temperatures (Liu et al., 2017). However, during periods of extreme weather caused by tropical cyclones, small and medium-sized rivers can transport large amounts of sediment to estuary areas (Tang et al., 2021). From 1966 to 2020, tropical cyclones contributed an average of 19.31% to the sediment load of the Nanliu River (Yang et al., 2023). The contribution of tropical cyclones to the sediment transport of large rivers was even greater; during the period of 1981—2005, tropical cyclones contributed between 15.2% and 31.7% to the sediment load of the Mekong River (Darby et al., 2016). It is evident that the extreme weather induced by tropical cyclones has a significant impact on the development of estuarine mangrove tidal flats.

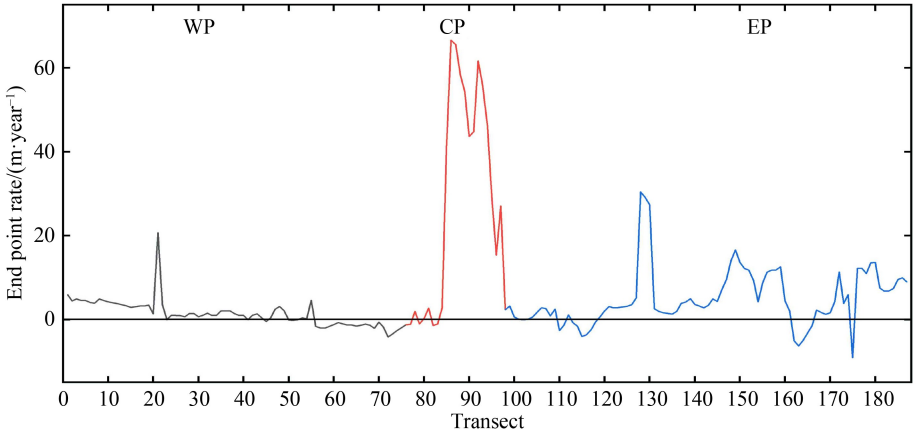

Fig. 14 Endpoint rate of the mudflat shoreline in the DDS from 1992 to 2021.

4.5 Impact of nature reserve establishment

Mangrove reserves play a crucial role in improving intertidal zone ecosystems (Turschwell et al., 2020). However, human activities also cause damage to the mangroves within the reserves (De Almeida et al., 2016). Studies have shown that the establishment and expansion of mangrove reserves in developing countries often do not follow scientific standards or appropriate techniques (Macedo et al., 2013), affecting the effectiveness of mangrove conservation. The DDS area is accompanied by the introduction and implementation of government policies related to mangrove conservation. Between 1987 and 2021, at a growth rate of 99.98%, the mangrove area in the DDS expanded from 225.90 to 451.76 ha (Fig. 3). This finding aligns with the findings of Lu et al. (2022), who indicated that the conservation effectiveness of the Shankou Mangrove Reserve increased by 25.2% from 1987 to 2019. However, due to the lack of awareness of mangrove conservation among the local people, the mangroves in the DDS were still strongly disturbed by human activities, leading to the mangrove ecosystem becoming more fragile from 1987 to 2021 (Fig. 6). In addition, from 1987 to 2021, *S. alterniflora* cumulatively encroached on 112.38 ha of mangroves, accounting for 41.69% of the mangrove loss. Human activities directly caused the cumulative encroachment of 157.18 ha of mangroves by woodland, arable land, construction land and bare land, aquaculture ponds, and bare flats, accounting for 58.31% of the mangrove loss (Table 7). Contrary to our research findings, the expansion of construction land and aquaculture ponds was the main factor causing the loss of mangroves in the Dongzhaigang Mangrove Nature Reserve (Du et al., 2023). In Sembilang National Park, the expansion of aquaculture ponds was identified as the key factor leading to the degradation of mangroves (Hauser et al., 2017). Moreover, in the Sundarbans Reserved Forest and the Rufiji-Mafia-Kilwa Marine Ramsar Site, agricultural encroachment was the principal cause of mangrove degradation (Giri et al., 2007; Monga et al., 2022). There are similarities and differences in the causes of mangrove loss in different regions. When carrying out mangrove conservation, it is essential to fully integrate modern information technologies such as remote sensing with manual field surveys. Adhering to standards, long-term information collection, and observation of various environmental factors should be conducted. Simultaneously, related predictive models based on existing observational data can be developed and utilized to forecast the evolutionary trends of mangrove wetland ecosystems. This will be useful to promptly respond to and prevent the influence of natural stress factors such as biological invasions, rising sea levels, and sharp decreases in river sediment, as well as human activities such as the expansion of construction land, arable land, and aquaculture ponds, which contribute to the deterioration of mangroves. Additionally, the primary task for the ecological restoration of the DDS mangroves at the current stage should involve intensifying human intervention in the growth and reproduction of *S. alterniflora* to curb its invasive expansion, and to systematically and extensively eradicate it, thereby reducing its spatial distribution.

4.6 Dynamic change patterns of the mangrove forests

Under the combined influence of the factors discussed above, the mangrove forests in the DDS underwent distinct expansion phases: initially, a rapid growth phase was observed, followed by a slow expansion phase, and eventually a stagnation phase (Fig. 15). The first phase lasted from 1987 to 1996 (Figs. 15(a) and 15(b)). During this period, large areas of bare mudflats dominated the WP and CP of the DDS. The expansion of mangroves was limited due to a lack of nutrients such as nitrogen, phosphorus, and potassium in the mudflat sediments (Reef et al., 2010; Twilley et al., 2017), which restricted the comprehensive colonization of these mangroves across the various potential forestation zones. However, as the mangrove trees on the mudflats continued to grow, their structures reduced water dynamics and enhanced the adsorption and interception of suspended sediment and nutrients in the water (Zhou et al., 2016; Wang et al., 2023). Additionally, the return of fallen organic matter to mudflats gradually improved the growth environment, leading to the continuous expansion of mangroves into mudflat areas. Therefore, the expansion of mangrove forests in the WP and CP was relatively rapid (Figs. 15(a) and 15(b)). In turn, the seeds of *S. alterniflora* are tiny, allowing them to effectively remain in the mudflat pores, and they can grow normally in clay, loam, and sandy soils (Deng et al., 2010). Consequently, *S. alterniflora* grew at the forefront of the mangrove flats in the transitional area between the CP and EP.

In the second phase, from 1997 to 2011 (Figs. 15(b) and 15(c)), the area of aquaculture ponds expanded, leading to intensified tidal dynamics. The embryonic establishment of mangroves on bare tidal flats faced increased resistance. Young mangrove forests also experienced heightened resistance to the absorption of

Table 7 The cumulative encroachment of other land types on mangrove forests from 1987 to 2021

	Woodland	Cultivated land	Construction land and bare land	Aquaculture ponds	*S. Alterniflora*	Bare tidal flat
Area/ha	13.99	8.65	21.32	25.47	112.38	87.75
Proportion/%	5.19	3.21	7.91	9.45	41.69	32.55

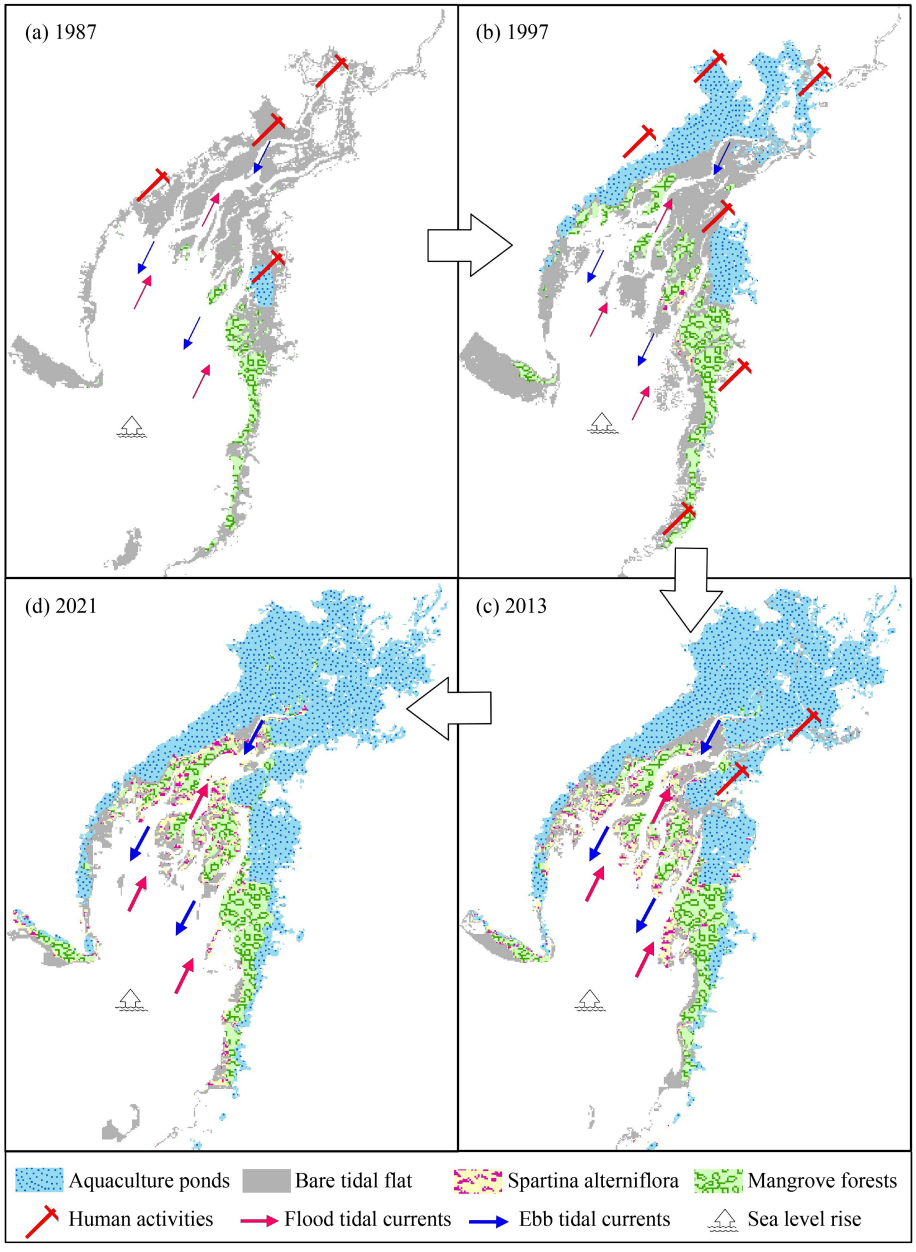

Fig. 15 Expansion model of mangrove forests in the DDS from 1987 to 2021.

suspended sediments and nutrients from water, which limited their growth and expansion. Furthermore, *S. alterniflora* has a unique mode of reproduction (Pan et al., 2016). Additionally, the amount of nutrients such as nitrogen and phosphorus entering the tidal flats during ebb tide increased, accelerating the invasion of *S. alterniflora* (Liu et al., 2021). During this phase, *S. alterniflora* rapidly occupied tidal flats across various regions, intruded into mangrove patches, restricted the spatial expansion of mangroves, and led to the fragmentation and extinction of local mangrove patches.

In the third phase, from 2013 to 2021 (Figs. 15(c) and 15(d)), the expansion of *S. alterniflora* stabilized due to human intervention and management. *S. alterniflora* surrounded mangrove patches and invaded sparser areas of mangroves, which continued to degrade and disappear. Concurrently, the area of aquaculture ponds reached a stable phase, and the regional water dynamics remained strong. As a result, the spatial expansion of mangroves stagnated, indicating that the mangrove ecosystem is fragile.

5 Conclusions

The dynamic changes in the mangrove forests in the DDS, as an integral part of the wetland ecosystem of the Guangxi Shankou Mangrove National Nature Reserve, were threatened by factors such as regional sea level rise, rapid expansion of aquaculture ponds, large-scale

invasion by *S. alterniflora*, spread of built areas, and tidal flat economic activities. This study, utilizing the GEE cloud platform and the random forest algorithm, investigated the dynamic changes in mangrove forests in the DDS and their underlying causes from 1987 to 2021. The main findings are as follows.

1) From 1987 to 2021, the mangrove area in the DDS expanded from 225.90 to 451.76 ha. The dynamic changes in mangrove forests in the DDS, as well as in the WP and CP, exhibited three distinct phases: a rapid expansion stage from 1987 to 1996, a slow expansion stage from 1997 to 2011, and a stagnation stage from 2013 to 2021. However, as the mangrove forests expanded, their patches became increasingly scattered and fragmented, and the distribution of mangroves in the DDS tended toward fragmentation.

2) The establishment of mangrove nature reserves had a significant positive impact on the restoration and expansion of mangrove forests in the DDS. However, the construction of aquaculture ponds, the invasion of *S. alterniflora*, the expansion of construction land, and seafood collection during ebb tide were among a series of natural and anthropogenic activities that inhibited the comprehensive expansion of mangroves and led to their fragmentation. Additionally, regional sea level rise did not negatively impact the seaward expansion of mangroves in the DDS.

3) In the process of restoring and protecting mangroves, it is suggested to combine modern information technologies such as remote sensing with manual field surveys, collect and observe long-term information on various environmental factors according to standards, and simultaneously develop and utilize related predictive models based on existing observational data to forecast the evolution trends of mangrove wetland ecosystems, to be able promptly respond to and prevent their deterioration.

Acknowledgments This research was supported by the National Natural Science Key Foundation of China (NSFC) (Grant Nos. 41930537 and 42366009), and Marine Science Program for Guangxi First-Class Discipline, Beibu Gulf University.

Competing interests The authors declare that they have no competing interests.

References

Abdul Azeez S, Gnanappazham L, Muraleedharan K R, Revichandran C, Sebin J, Seena G, Jubin T (2022). Multi-decadal changes of mangrove forest and its response to the tidal dynamics of thane creek, Mumbai. J Sea Res, 180: 102162

Afonso F, Palma C, Brito A C, Chainho P, de Lima R, Heumüller J A, Ribeiro F, Félix P M (2023). Metal and semimetal loadings in sediments and water from mangrove ecosystems: a preliminary assessment of anthropogenic enrichment in São Tomé island (central Africa). Chemosphere, 334: 138973

Amani M, Ghorbanian A, Ahmadi S A, Kakooei M, Moghimi A, Mirmazloumi S M, Moghaddam S H A, Mahdavi S, Ghahremanloo M, Parsian S, Wu Q, Brisco B (2020). Google earth engine cloud computing platform for remote sensing big data applications: a comprehensive review. IEEE J Sel Top Appl Earth Obs Remote Sens, 13: 5326–5350

Asbridge E, Lucas R, Rogers K, Accad A (2018). The extent of mangrove change and potential for recovery following severe Tropical Cyclone Yasi, Hinchinbrook Island, Queensland, Australia. Ecol Evol, 8(21): 10416–10434

Baloloy A B, Blanco A C, Sta. Ana R R C S, Nadaoka K (2020). Development and application of a new mangrove vegetation index (MVI) for rapid and accurate mangrove mapping. ISPRS J Photogramm Remote Sens, 166: 95–117

Bimrah K, Dasgupta R, Hashimoto S, Saizen I, Dhyani S (2022). Ecosystem services of mangroves: A systematic review and synthesis of contemporary scientific literature. Sustainability (Basel), 14(19): 12051

Bunting P, Rosenqvist A, Hilarides L, Lucas R M, Thomas N, Tadono T, Worthington T A, Spalding M, Murray N J, Rebelo L M (2022). Global mangrove extent change 1996–2020: global mangrove watch version 3.0. Remote Sens (Basel), 14(15): 3657

Chen Q, Ma K M (2015). Research overview and trend on biological invasion in mangrove forests. Acta Phytoecol Sin, 39(3): 283–299

Darby S E, Hackney C R, Leyland J, Kummu M, Lauri H, Parsons D R, Best J L, Nicholas A P, Aalto R (2016). Fluvial sediment supply to a mega-delta reduced by shifting tropical-cyclone activity. Nature, 539(7628): 276–279

De Almeida L T, Olímpio J L S, Pantalena A F, De Almeida B S, De Oliveira Soares M (2016). Evaluating ten years of management effectiveness in a mangrove protected area. Ocean Coast Manage, 125: 29–37

Deng Z F, Xie X L, Wang Z S, An S Q (2010). Effects of substrate and water level on the growth of invasive species *Spartina alterniflora*. Chinese J Eco, 29(02): 256–260 (in Chinese)

Donato D C, Kauffman J B, Murdiyarso D, Kurnianto S, Stidham M, Kanninen M (2011). Mangroves among the most carbon-rich forests in the tropics. Nat Geosci, 4(5): 293–297

Du C, Khan S, Ke Y, Zhou D (2023). Assessment of spatiotemporal dynamics of mangrove in five typical mangrove reserve wetlands in Asia, Africa and Oceania. Diversity (Basel), 15(2): 148

Duke N C, Meynecke J O, Dittmann S, Ellison A M, Anger K, Berger U, Cannicci S, Diele K, Ewel K C, Field C D, Koedam N, Lee S Y, Marchand C, Nordhaus I, Dahdouh-Guebas F (2007). A world without mangroves. Science, 317(5834): 41–42

Feller I C, Lovelock C E, Berger U, McKee K L, Joye S B, Ball M C (2010). Biocomplexity in mangrove ecosystems. Annu Rev Mar Sci, 2(1): 395–417

Feng Z, Tan G, Xia J, Shu C, Chen P, Wu M, Wu X (2020). Dynamics of mangrove forests in Shenzhen Bay in response to natural and anthropogenic factors from 1988 to 2017. J Hydrol (Amst), 591: 125271

Gao G F, Li P F, Shen Z J, Qin Y Y, Zhang X M, Ghoto K, Zhu X Y, Zheng H L (2018). Exotic Spartina alterniflora invasion increases

CH_4 while reduces CO_2 emissions from mangrove wetland soils in southeastern China. Sci Rep, 8(1): 9243

Getzner M, Islam M S (2020). Ecosystem services of mangrove forests: Results of a meta-analysis of economic values. Int J Environ Res Public Health, 17(16): 5830

Gilani H, Naz H I, Arshad M, Nazim K, Akram U, Abrar A, Asif M (2021). Evaluating mangrove conservation and sustainability through spatiotemporal (1990–2020) mangrove cover change analysis in Pakistan. Estuar Coast Shelf Sci, 249: 107128

Giri C, Pengra B, Zhu Z, Singh A, Tieszen L L (2007). Monitoring mangrove forest dynamics of the Sundarbans in Bangladesh and India using multi-temporal satellite data from 1973 to 2000. Estuar Coast Shelf Sci, 73(1−2): 91–100

Gitau P N, Duvail S, Verschuren D (2023). Evaluating the combined impacts of hydrological change, coastal dynamics and human activity on mangrove cover and health in the Tana River delta, Kenya. Regional Studies in Marine Science, 61: 102898

Gorelick N, Hancher M, Dixon M, Ilyushchenko S, Thau D, Moore R (2017). Google Earth Engine: planetary-scale geospatial analysis for everyone. Remote Sens Environ, 202: 18–27

Hauser L T, Nguyen Vu G, Nguyen B A, Dade E, Nguyen H M, Nguyen T T Q, Le T Q, Vu L H, Tong A T H, Pham H V (2017). Uncovering the spatio-temporal dynamics of land cover change and fragmentation of mangroves in the Ca Mau peninsula, Vietnam using multi-temporal SPOT satellite imagery (2004–2013). Appl Geogr, 86: 197–207

He Q F, Fan H Q, Mo Z C, Wang X, Shen W H (2012). Impacts of digging *Phascolosoma esculenta* on the growth of mangrove *Avicennia marina* seedlings: a simulation study. Chinese J App Eco, 23(04): 947–952 (in Chinese)

Huang X, Yuan J J, Wang X P, Yue K K, Zhang Q (2022). Dynamics of mangrove change: insights from 30-year observations of Maowei Sea. J Mar Sci, 40(03): 132–141 (in Chinese)

Jayanthi M, Samynathan M, Thirumurthy S, Duraismay M, Kabiraj S, Vijayakumar S, Panigrahi A, Kumaran M, Muralidhar M (2022). Is aquaculture development responsible for mangrove conversion in India?-A geospatial study to assess the influence of natural and anthropogenic factors on mangroves in the last three decades. Aquaculture, 561: 738696

Jia M, Wang Z, Zhang Y, Ren C, Song K (2015). Landsat-based estimation of mangrove forest loss and restoration in Guangxi province, China, influenced by human and natural factors. IEEE J Sel Top Appl Earth Obs Remote Sens, 8(1): 311–323

Jiang X H, Xie L J, Ye S Y, Zhou P, Pei L X, Chen H, Zhao L H (2022). Responses of photosynthetic charactristics of *Phragmites australis* and *Spartina alterniflora* to the simulated warming in Jiangsu coastal wetlands. Acta Ecol Sin, 42(19): 7760–7772 (in Chinese)

Kirwan M L, Megonigal J P (2013). Tidal wetland stability in the face of human impacts and sea-level rise. Nature, 504(7478): 53–60

Krauss K W, From A S, Doyle T W, Doyle T J, Barry M J (2011). Sea-level rise and landscape change influence mangrove encroachment onto marsh in the Ten Thousand Islands region of Florida, USA. J Coast Conserv, 15(4): 629–638

Le Minor M, Bartzke G, Zimmer M, Gillis L, Helfer V, Huhn K (2019). Numerical modelling of hydraulics and sediment dynamics around mangrove seedlings: Implications for mangrove establishment and reforestation. Estuar Coast Shelf Sci, 217: 81–95

Lee S Y, Hamilton S, Barbier E B, Primavera J, Lewis R R III (2019). Better restoration policies are needed to conserve mangrove ecosystems. Nat Ecol Evol, 3(6): 870–872

Li S, Dai Z, Ge Z, Xie H, Huang H (2014). Research on the changes of the ecological environment disasters along the northern Beibu Gulf. J Catastroph, 29(4): 43–47 (in Chinese)

Liu H Y, Zhou Y, Guo Z R, Dai L J, Wang C, Wang G, Li Y F (2021). A conceptual ecological model for large-scale salt marsh restoration: a case study of Yancheng. Chinese J Eco, 40(01): 278–291 (in Chinese)

Liu M, Mao D, Wang Z, Li L, Man W, Jia M, Ren C, Zhang Y (2018). Rapid invasion of *Spartina alterniflora* in the coastal zone of mainland China: new observations from Landsat OLI images. Remote Sens (Basel), 10(12): 1933

Liu T, Tao Y, Liu Y (2017). Mangrove swamp expansion controlled by climate since 1988: a case study in the Nanliu River Estuary, Guangxi, Southwest China. Acta Oceanol Sin, 36(12): 11–17

Long C, Dai Z, Wang R, Lou Y, Zhou X, Li S, Nie Y (2022). Dynamic changes in mangroves of the largest delta in northern Beibu Gulf, China: reasons and causes. For Ecol Manage, 504: 119855

Long C, Dai Z, Zhou X, Mei X, Mai Van C (2021). Mapping mangrove forests in the Red River Delta, Vietnam. For Ecol Manage, 483: 118910

Long J, Giri C, Primavera J, Trivedi M (2016). Damage and recovery assessment of the Philippines' mangroves following Super Typhoon Haiyan. Mar Pollut Bull, 109(2): 734–743

López-Medellín X, Ezcurra E, González-Abraham C, Hak J, Santiago L S, Sickman J O (2011). Oceanographic anomalies and sea‐level rise drive mangroves inland in the Pacific coast of Mexico. J Veg Sci, 22(1): 143–151

Lovelock C E, Feller I C, Reef R, Hickey S, Ball M C (2017). Mangrove dieback during fluctuating sea levels. Sci Rep, 7(1): 1680

Lu C, Li L, Wang Z, Su Y, Su Y, Huang Y, Jia M, Mao D (2022). The national nature reserves in China: are they effective in conserving mangroves. Ecol Indic, 142: 109265

Lu C, Liu J, Jia M, Liu M, Man W, Fu W, Zhong L, Lin X, Su Y, Gao Y (2018). Dynamic analysis of mangrove forests based on an optimal segmentation scale model and multi-seasonal images in Quanzhou Bay, China. Remote Sens (Basel), 10(12): 2020

Macedo H S, Vivacqua M, Rodrigues H C L, Gerhardinger L C (2013). Governing wide coastal-marine protected territories: a governance analysis of the Baleia Franca Environmental Protection Area in South Brazil. Mar Policy, 41: 118–125

McGarigal K, Marks B J (1995). Spatial pattern analysis program for quantifying landscape structure. Gen. Tech. Rep. PNW-GTR-351. US Department of Agriculture, Forest Service, Pacific Northwest Research Station, 1–122

Monga E, Mangora M M, Trettin C C (2022). Impact of mangrove planting on forest biomass carbon and other structural attributes in the Rufiji Delta, Tanzania. Glob Ecol Conserv, 35: e02100

Morocho R, González I, Ferreira T O, Otero X L (2022). Mangrove forests in Ecuador: a two-decade analysis. Forests, 13(5): 656

Morrissette H K, Baez S K, Beers L, Bood N, Martinez N D, Novelo K, Andrews G, Balan L, Beers C S, Betancourt S A, Blanco R, Bowden E, Burns-Perez V, Carcamo M, Chevez L, Crooks S, Feller I C, Galvez G, Garbutt K, Gongora R, Grijalva E, Lefcheck J, Mahung A, Mattis C, McKoy T, McLaughlin D, Meza J, Pott E, Ramirez G, Ramnarace V, Rash A, Rosado S, Santos H, Santoya L, Sosa W, Ugarte G, Viamil J, Young A, Young J, Canty S W (2023). Belize Blue Carbon: establishing a national carbon stock estimate for mangrove ecosystems. Sci Total Environ, 870: 161829

Mou N X, Liu W B, Wang H Y, Dai H L (2012). ArcGIS 10 Tutorial: from Beginner to Master. Beijing: Surveying and Mapping Press, 311–318

Murillo-Sandoval P J, Fatoyinbo L, Simard M (2022). Mangroves cover change trajectories 1984–2020: the gradual decrease of mangroves in Colombia. Front Mar Sci, 9: 892946

Nguyen H T T, Hardy G E, Le T V, Nguyen H Q, Nguyen H H, Nguyen T V, Dell B (2021). Mangrove forest landcover changes in coastal Vietnam: a case study from 1973 to 2020 in Thanh Hoa and Nghe An provinces. Forests, 12(5): 637

Ofori S A, Kodikara S K, Jayatissa L P, Madarasinghe S K, Nijamdeen T M, Dahdouh-Guebas F (2023). What is the ecological footprint of aquaculture after 5 decades of competition between mangrove conservation and shrimp farm development. Aquat Conserv, 33(1): 15–28

Osorio-Olvera L, Rioja-Nieto R, Torres-Irineo E, Guerra-Martínez F (2023). Natural Protected Areas effect on the cover change rate of mangrove forests in the Yucatan Peninsula, Mexico. Wetlands, 43(5): 52

Pan L H, Shi X F, Tao Y C, Fan H Q, Mo Z C (2016). Distribution and expansion of *Spartina alterniflora* in coastal tidal zone, Guangxi. Wetland Sci, 14(4): 464–470 (in Chinese)

Phan M H, Stive M J (2022). Managing mangroves and coastal land cover in the Mekong Delta. Ocean Coast Manage, 219: 106013

Polidoro B A, Carpenter K E, Collins L, Duke N C, Ellison A M, Ellison J C, Farnsworth E J, Fernando E S, Kathiresan K, Koedam N E, Livingstone S R, Miyagi T, Moore G E, Ngoc Nam V, Ong J E, Primavera J H, Salmo S G III, Sanciangco J C, Sukardjo S, Wang Y, Yong J W H (2010). The loss of species: mangrove extinction risk and geographic areas of global concern. PLoS One, 5(4): e10095

Qi Y, Liu D, Huang X, Pu X (2019). Topographical mapping of a bare tidal flat outside a mangrove area based on the waterline method and an iterative hydrodynamic model: a case study of Yingluo Bay, South China. Mar Geod, 42(3): 263–285

Reef R, Feller I C, Lovelock C E (2010). Nutrition of mangroves. Tree Physiol, 30(9): 1148–1160

Rouse J W, Haas R H, Schell J A, Deering D W (1974). Monitoring vegetation systems in the Great Plains with ERTS. NASA Spec Publ, 351(1): 309

Rull V (2023). Rise and fall of Caribbean mangroves. Sci Total Environ, 885: 163851

Shen H K, Zhao B Y, Chen M Y, Huang R Y, Yu K F, Liang W (2022). Changes of the area of *Spartina alterniflora* and mangroves in Guangxi Shankou Mangrove National Nature Reserve from 1995 to 2019. Chinese J App Eco, 33(2): 397–404

Shi M, Li H, Jia M (2023). Spatio-temporal variations in mangrove forests in the Shankou Mangrove Nature Reserve based on the GEE cloud platform and Landsat data. Remote Sens Nat Resour, 35(2): 61–69 (in Chinese)

Simard M, Fatoyinbo L, Smetanka C, Rivera-Monroy V H, Castañeda-Moya E, Thomas N, Van der Stocken T (2019). Mangrove canopy height globally related to precipitation, temperature and cyclone frequency. Nat Geosci, 12(1): 40–45

Sippo J Z, Lovelock C E, Santos I R, Sanders C J, Maher D T (2018). Mangrove mortality in a changing climate: an overview. Estuar Coast Shelf Sci, 215: 241–249

Soeprobowati T R, Sularto R B, Hadiyanto H, Puryono S, Rahim A, Jumari J, Gell P (2024). The carbon stock potential of the restored mangrove ecosystem of Pasarbanggi, Rembang, Central Java. Mar Environ Res, 193: 106257

Tang R, Dai Z, Zhou X, Li S (2021). Tropical cyclone-induced water and suspended sediment discharge delivered by mountainous rivers into the Beibu Gulf, south China. Geomorphology, 389: 107844

Tinh P H, MacKenzie R A, Hung T D, Hanh N T H, Hanh N H, Manh D Q, Ha H T, Tuan M S (2022). Distribution and drivers of Vietnam mangrove deforestation from 1995 to 2019. Mitig Adapt Strategies Glob Change, 27(4): 29

Tran T V, Reef R, Zhu X (2022). A review of spectral indices for mangrove remote sensing. Remote Sens (Basel), 14(19): 4868

Turschwell M P, Tulloch V J, Sievers M, Pearson R M, Andradi-Brown D A, Ahmadia G N, Connolly R M, Bryan-Brown D, Lopez-Marcano S, Adame M F, Brown C J (2020). Multi-scale estimation of the effects of pressures and drivers on mangrove forest loss globally. Biol Conserv, 247: 108637

Twilley R R, Castañeda-Moya E, Rivera-Monroy V H, Rovai A (2017). Productivity and carbon dynamics in mangrove wetlands. In: Rivera-Monroy V H, Lee S Y, Kristensen E, Twilley R R, eds. Mangrove Ecosystems: A Global Biogeographic Perspective: Structure, Function, and Services, 113–162

Walcker R, Laplanche C, Herteman M, Lambs L, Fromard F (2019). Damages caused by hurricane Irma in the human-degraded mangroves of Saint Martin (Caribbean). Sci Rep, 9(1): 18971

Wang G, Guan D, Xiao L, Peart M R, Zhang H, Singh M (2019b). Changes in mangrove community structures affecting sediment carbon content in Yingluo Bay of south China. Mar Pollut Bull, 149: 110581

Wang G, Guan D, Zhang Q, Peart M R, Chen Y, Peng Y, Ling X (2014). Spatial patterns of biomass and soil attributes in an estuarine mangrove forest (Yingluo Bay, south China). Eur J For Res, 133(6): 993–1005

Wang R, Dai Z, Huang H, Liang X, Zhou X, Ge Z, Hu B (2023). Dramatic changes in the horizontal structure of mangrove forests in the largest delta of the northern Beibu Gulf, China. Acta Oceanol Sin, 42(7): 116–123

Wang W, Sardans J, Wang C, Zeng C, Tong C, Chen G, Huang J, Pan H, Peguero G, Vallicrosa H, Peñuelas J (2019a). The response of stocks of C, N, and P to plant invasion in the coastal wetlands of China. Glob Change Biol, 25(2): 733–743

Wang Z, Liu K, Cao J, Peng L, Wen X (2022). Annual change analysis of mangrove forests in China during 1986–2021 based on Google

Earth engine. Forests, 13(9): 1489

Xia P, Meng X W, Feng A P, Li Z, Yang G (2015). Sediment compaction rates in mangrove swamps of Guangxi and its mangrove migration response to sea-level rise. Acta Sediment Sin, 33(3): 551–560

Xiong Y, Dai Z, Long C, Liang X, Lou Y, Mei X, Nguyen B, Cheng J (2024). Machine Learning-Based examination of recent mangrove forest changes in the western Irrawaddy River Delta, Southeast Asia. Catena, 234: 107601

Xu H Q (2005). A study on information extraction of water body with the modified normalized difference water index (MNDWI). Nation Remote Sens Bull, 9(5): 589–595 (in Chinese)

Yang J Y, Luo F S, Wang A J, Yu D S (2020). Comprehensive evaluation for silted bay restoration: a case study in Xiamen Bay. J App Oceanograph, 39(3): 389–399 (in Chinese)

Yang X, Li S, Xu S, Yu C, Pan J (2023). Variations in water and sediments of the Nanliu River flowing into the sea under the influence of extreme weather in the past 60 years. J Tropical Oceanograph, 42(4): 91–103 (in Chinese)

Yoshikai M, Nakamura T, Bautista D M, Herrera E C, Baloloy A, Suwa R, Basina R, Primavera-Tirol Y H, Blanco A C, Nadaoka K (2022). Field measurement and prediction of drag in a planted Rhizophora mangrove forest. J Geophys Res: Oceans, 127(11): e2021JC018320

Yue W, Li C T, Lin Y Y, Feng T Q, Wang L R (2023). History and prospect on ecological restoration of mangroves on Qi'ao Island, Zhuhai. J Guangdong Ocean Univ, 43(2): 135–140 (in Chinese)

Zha Y, Gao J, Ni S (2003). Use of normalized difference built-up index in automatically mapping urban areas from TM imagery. Int J Remote Sens, 24(3): 583–594

Zhang W, Chen Z H, Wang J K (2015). Monitoring the areal variation of mangrove in Beibu Gulf coast of Guangxi China with remote sensing data. J Guangxi U (Nat Sci Ed), 40(6): 1570–1576 (in Chinese)

Zhang Z, Ahmed M R, Zhang Q, Li Y, Li Y (2023). Monitoring of 35-year mangrove wetland change dynamics and agents in the sundarbans using temporal consistency checking. Remote Sens (Basel), 15(3): 625

Zhao C, Qin C Z, Wang Z, Mao D, Wang Y, Jia M (2022). Decision surface optimization in mapping exotic mangrove species (*Sonneratia apetala*) across latitudinal coastal areas of China. ISPRS J Photogramm Remote Sens, 193: 269–283

Zhou X, Dai Z, Carniello L, Long C, Wang R, Luo J, Huang Z (2022). Linkage between mangrove wetland dynamics and wave attenuation during a storm–A case study of the Nanliu Delta, China. Mar Geol, 454: 106946

Zhou Z, Ye Q, Coco G (2016). A one-dimensional biomorphodynamic model of tidal flats: sediment sorting, marsh distribution, and carbon accumulation under sea level rise. Adv Water Resour, 93: 288–302